ORIGINAL ARTICLE

Clinical implications of ^{18}F-sodium fluoride uptake in subclinical aortic valve calcification: Its relation to coronary atherosclerosis and its predictive value

Yumiko Nakamoto, MD,[a] Toshiro Kitagawa, MD, PhD,[a] Ko Sasaki, RT,[b]
Fuminari Tatsugami, MD, PhD,[c] Kazuo Awai, MD, PhD,[c]
Yutaka Hirokawa, MD, PhD,[b] and Yasuki Kihara, MD, PhD[a]

[a] Department of Cardiovascular Medicine, Hiroshima University Graduate School of Biomedical and Health Sciences, Hiroshima, Japan
[b] Hiroshima Heiwa Clinic, Hiroshima, Japan
[c] Department of Diagnostic Radiology, Hiroshima University Hospital, Hiroshima, Japan

Background. Uptake of ^{18}F-sodium fluoride (^{18}F-NaF) on positron emission tomography (PET) reflects active calcification. Application of this technique in the early phase of aortic valve calcification (AVC) is of clinical interest. We investigated clinical implications of ^{18}F-NaF uptake in subclinical AVC evaluated simultaneously with coronary atherosclerosis, and the utility of ^{18}F-NaF uptake in predicting AVC progression.

Methods. We studied 25 patients with subclinical AVC and coronary plaques detected on computed tomography (CT) who underwent ^{18}F-NaF PET/CT. AVC score, volume, mean density, and the presence of high-risk coronary plaque were evaluated on CT in each patient. Focal ^{18}F-NaF uptake in AVC and in coronary plaques was quantified with the maximum tissue-to-background ratio (TBR$_{max}$).

Results. There were positive correlations between AVC TBR$_{max}$ (A-TBR$_{max}$) and AVC parameters on CT. The 14 patients with high-risk coronary plaque had significantly higher A-TBR$_{max}$ than those without such plaque (1.60 ± 0.18 vs 1.42 ± 0.13, respectively; $P = 0.012$). A-TBR$_{max}$ positively correlated with maximum TBR$_{max}$ of coronary plaque per patient ($r = 0.55$, $P = 0.0043$). In the 11 patients who underwent follow-up CT scan, A-TBR$_{max}$ positively correlated with subsequent increase in AVC score ($r = 0.74$, $P = 0.0091$).

Conclusion. Our ^{18}F-NaF PET- and CT-based data indicate relationships between calcification activity in subclinical AVC and characteristics of coronary atherosclerosis. ^{18}F-NaF PET may provide new information regarding molecular conditions and future progression of subclinical AVC. (J Nucl Cardiol 2021;28:1522–31.)

Key Words: Valvular heart disease · CT · PET · metabolism imaging agents

Reprint requests: Toshiro Kitagawa, MD, PhD, Department of Cardiovascular Medicine, Hiroshima University Graduate School of Biomedical and Health Sciences, 1-2-3 Kasumi, Minami-ku, Hiroshima734-8551, Japan; *toshirok@hiroshima-u.ac.jp*

1071-3581/$34.00

Abbreviations

AS	Aortic valve stenosis
A-TBR$_{max}$	Aortic valve calcification maximum tissue-to-background ratio
AVC	Aortic valve calcification
CCTA	Coronary-computed tomography angiography
CT	Computed tomography
^{18}F-NaF	^{18}F-sodium fluoride
M-TBR$_{max}$	Maximum tissue-to-background ratio per patient in any coronary atherosclerotic lesion
PET	Positron emission tomography
SUV$_{max}$	Maximum standardized uptake value
TBR$_{max}$	Maximum tissue-to-background ratio

INTRODUCTION

Aortic valve calcification (AVC) is a main etiological mechanism of aortic valve stenosis (AS). Computed tomography (CT) and echocardiography are used to measure established, macro-calcification of the aortic valve. However, these modalities cannot directly assess ongoing calcification activity, which is considered the main driver of disease progression. Although the amount of established calcium in aortic valves correlates with disease severity and poor prognosis,[1] accurate prediction of AS progression remains challenging in the clinical setting.

Recently, ^{18}F-sodium fluoride (^{18}F-NaF) positron emission tomography (PET) has been applied to atherosclerosis and cardiovascular diseases, including carotid artery disease, coronary artery disease, and valvular heart disease.[2-4] The ^{18}F-NaF tracer binds to hydroxyapatite, which is the central component of tissue calcification and is laid down during the earliest and active stages of mineralization. An association between osteogenesis and inflammation has been suggested in the development of atherosclerosis,[5,6] and the pathophysiology of calcific AS shares many similarities with atherosclerosis, including lipid deposition, inflammation, and calcification.[7] Thus, simultaneous assessment of metabolic activity in AVC and in coronary atherosclerosis as indicated by ^{18}F-NaF uptake may provide new insight into the pathophysiology of AVC.

In patients with AS, valvular ^{18}F-NaF uptake correlates with histological markers of active calcification and predicts subsequent progression in calcium scores of the aortic valves on CT.[8] Valvular ^{18}F-NaF uptake is considered a marker of calcification activity in the heart valves; investigation of its significance in the early phase of valve disease may help prevent progression to AS. However, this aspect has not been studied.

In this study, we simultaneously evaluated ^{18}F-NaF uptake in subclinical AVC and in coronary atherosclerosis detected and assessed with CT examination. Additionally, we evaluated the utility of ^{18}F-NaF uptake in predicting AVC progression.

MATERIALS AND METHODS

Study Participants

This was a post hoc analysis of our previous study.[9,10] Between June 2014 and December 2018, a total of 44 patients with known or suspected coronary artery disease underwent both cardiac CT and ^{18}F-NaF PET/CT. All patients were referred for cardiac CT to evaluate and diagnose coronary artery disease and had at least one coronary atherosclerotic lesion detected on coronary CT angiography (CCTA) in segments > 2-mm in diameter according to the Society of Cardiovascular Computed Tomography's 18-segment model.[11] We retrospectively reviewed these patients and identified 25 with AVC verified on non-contrast CT images for further analysis in this study. None of these patients had clinical AS, defined as peak aortic valve velocity $\geq$ 2.0 m/s on Doppler echocardiography. Exclusion criteria included the presence of cardiac arrhythmias (i.e., atrial fibrillation, frequent paroxysmal premature beats), contraindications to iodinated contrast medium, unstable hemodynamic conditions, and ongoing myocardial infarction or unstable angina. Patients receiving dialysis were also excluded, which would have been a potentially confounding factor in the analysis of coronary calcification. We collected clinical information, including coronary risk factors and history of myocardial infarction or unstable angina. History of myocardial infarction or unstable angina was determined as explained in our previous report.[9]

Our hospital's ethics committee approved the study protocol; written informed consent was obtained from all patients. The study protocol has been published in the Japan UMIN Clinical Trials Registry (ID: UMIN000031134).

Cardiac CT Protocol and Image Analysis

All patients underwent cardiac CT with a 320-detector row CT scanner (Aquilion ONE; Canon Medical Systems, Otawara, Japan), as described in our previous report.[9] Briefly, a non-contrast scan was performed to measure the coronary calcium score and AVC score according to the standard Agatston method (slice thickness, 3.0 mm; maximum tube current, 270 mA; tube voltage, 120 kV). The data set for CCTA was acquired with the HeartNAVI system (collimation, 320×0.5 mm^2; tube current, 350-580 mA; tube voltage, 120 kV; Canon Medical Systems) with retrospective electrocardiography gating. The mean effective radiation dose

according to the dose-length product was 8 mSv per patient. All reconstructed CT image data were transferred to an offline workstation (Advantage Workstation Ver. 4.2; GE Healthcare, Waukesha, WI, USA). Two blinded independent observers performed post-processing and image analysis.

AVC was defined as a calcification lesion (structure with a CT density $\geq$ 130 Hounsfield units) just inferior to the origin of the right coronary arteries and located at the aortic leaflets, including the valvular point of attachment.[12] In addition to the measurement of AVC score, the extent of AVC was evaluated quantitatively on non-contrast CT images. The CT density was determined by placing five regions of interest in the AVC and documenting the mean value of all the regions of interest in each patient. The total volume of AVC in each patient was measured using a dedicated software (Smartscore, version 4.0, GE Healthcare).

On CCTA images, the coronary lumen for stenosis and atherosclerotic lesions in all coronary segments > 2-mm in diameter were evaluated as in our previous reports.[9,10] Lumen stenosis $\geq$ 70% in any vessel or $\geq$ 50% in the left main coronary artery was considered clinically obstructive. In each patient, the presence or absence of high-risk plaque was determined, which was defined as coronary plaques with a Low Density (< 30 Hounsfield units) and High Remodeling Index (> 1.1). Those were reported to be high-risk characteristics of coronary plaques resulting in acute coronary syndrome.[13,14] If the initial assessments of coronary stenosis and high-risk plaque differed between the two independent observers, agreement was reached by consensus.

18F-NaF PET/CT Protocol and Image Analysis

Within 1 month after cardiac CT scan, all patients underwent combined PET/CT imaging with a hybrid scanner (Discovery ST Elite-Performance, GE Healthcare), as in our previous report.[9] Briefly, after intravenous administration of a target dose of 370 MBq 18F-NaF and a 60-minutes rest, a non-contrast CT scan for attenuation correction and an electrocardiogram-gated emission PET scan of the thorax (25-minutes acquisition using the three-dimensional mode) were performed. An electrocardiogram-gated CT scan for fusion with PET images was then performed with the same axial coverage at 120 kV, 250 mA, and a slice thickness of 1.25 mm. The mean effective radiation dose for the CT scans (for attenuation correction and fusion) according to the dose-length product was 2 mSv per patient. The PET component of the combined imaging system allows simultaneous acquisition of 47 transaxial PET images with an interslice spacing of 3.27 mm in one bed position. The PET data were reconstructed with an ordered-subset expectation maximization iterative reconstruction algorithm called VUE Point Plus (21 subsets and two iterations). The reconstruction of PET data was performed in 8 multiple phases of the cardiac cycle, and the diastolic phase (62.5-75%) was used for analysis. Two experienced, blinded readers fused the PET and CT images and analyzed them with an offline workstation (Advantage Workstation Ver. 4.4; GE Healthcare).

Each AVC and coronary atherosclerotic lesion was identified visually using locations of calcium deposit and vessel branches on previously scanned CT images (non-contrast and CCTA images) as landmarks. The extent of valvular or arterial tracer uptake was standardized as described in previous reports.[3,4] To measure 18F-NaF uptake in AVC, a region of interest was drawn around each valvular calcification of the aortic valve on 3.27 mm axial slices and the maximum standardized uptake value (SUV_{max}, decay-corrected tissue concentration of the tracer divided by the injected dose per body weight) was determined. When multiple calcifications of the aortic valve were identified in a patient, the highest SUV_{max} was selected. The SUV_{max} of AVC was divided by an averaged mean SUV in the blood pool, derived from five circular regions of interest positioned in the center of the superior vena cava. This value was reported as the maximum tissue-to-background ratio (TBR_{max}), a measure of 18F-NaF uptake in AVC of each patient (A-TBR_{max}). To quantify 18F-NaF uptake in coronary atherosclerotic lesions, a region of interest was drawn around each lesion just beyond the discernible adventitial border and the SUV_{max} was measured. The SUV_{max} of each lesion was divided by the averaged mean SUV in the blood pool. This value was reported as the TBR_{max} for each coronary atherosclerotic lesion, a measure of 18F-NaF uptake. Additionally, maximum TBR_{max} per patient in any coronary atherosclerotic lesion was determined (M-TBR_{max}). If the coronary atherosclerotic lesions detected on the previously scanned coronary CT images could not be identified confidently on the fused PET/CT images, such lesions were excluded from the analysis via two-reader consensus.

Follow-Up Study on AVC Progression

A subgroup of the entire cohort underwent follow-up CT scan to evaluate the progression of AVC. More than 2 years after the first cardiac CT scan, a non-contrast CT scan was performed to measure the AVC score and the extent of AVC (CT density and volume), as in the first CT scan. Changes in the AVC score, density, and volume were calculated. The relationships between A-TBR_{max} and changes in AVC parameters on CT were then assessed.

Statistical Analysis

The coronary calcium score and AVC score, density (Hounsfield units), and volume (mm^3) on CT are expressed as the median (interquartile range); other continuous variables are expressed as the mean ± standard deviation. Student's t test or the Mann–Whitney U test was used for group comparisons of continuous variables. Interobserver variability of measured PET activities was determined by calculating the 95% confidence intervals for mean differences and 95% limits of agreement. Relationships between A-TBR_{max} and AVC parameters or subsequent changes in these parameters on CT were assessed by calculating Pearson's correlation. Linear regression was used for univariate and multivariate analyses; the value of standardized β was calculated to evaluate the relationship between A-TBR_{max} and clinical characteristics

or cardiac CT findings. *P* values < 0.05 were considered statistically significant. All statistical analyses were performed with JMP Pro 14 statistical software (SAS Institute Inc. Cary, NC, USA).

RESULTS

Baseline Information

Table 1 shows the baseline clinical characteristics of included patients. The peak aortic valve velocity on Doppler echocardiography was 1.4 ± 0.3 m/s (range 1.0-1.9 m/s). The AVC score, density, and volume on CT were 101 (11-171), 326 Hounsfield units (213-454 Hounsfield units), and 33 mm^3 (8-79 mm^3), respectively. The SUV$_{max}$ of AVC and A-TBR$_{max}$ on PET were 1.43 ± 0.28 and 1.52 ± 0.18, respectively. A total of 90 coronary atherosclerotic lesions (mean 3.6 ± 1.2 per patient; range, 2-6 lesions per patient) were analyzed; 19 of these were determined to be obstructive and 20 were defined as high-risk plaque on CCTA. Among the 25 patients, 14 had at least one lesion of obstructive coronary stenosis and 14 had high-risk plaque. The TBR$_{max}$ of all coronary atherosclerotic lesions and M-TBR$_{max}$ of all patients were 1.07 ± 0.22 and 1.23 ± 0.21, respectively. In the paired comparison, A-TBR$_{max}$ was significantly higher than M-TBR$_{max}$ (*P* < 0.0001).

We found good interobserver agreement for SUV$_{max}$ of AVC (mean difference, − 0.02; 95% confidence interval, − 0.09 to 0.06; 95% limits of agreement, − 0.39 to 0.35), and A-TBR$_{max}$ (mean difference, − 0.01; 95% confidence interval, − 0.10 to 0.07; 95% limits of agreement, − 0.40 to 0.37) (Supplementary

Table 1. Baseline clinical characteristics

Number of patients	25
Age (years)	70 ± 7
Male sex, n (%)	20 (80)
Body mass index (kg/m^2)	23 ± 3
Hypertension, n (%)	20 (80)
Dyslipidemia, n (%)	22 (88)
Diabetes mellitus, n (%)	14 (56)
Current smoking, n (%)	11 (44)
Statin therapy, n (%)	18 (72)
History of myocardial infarction or unstable angina, n (%)	16 (64)
Coronary stent implantation, n (%)	7 (29)
Coronary calcium score	314 (28-1147)

Coronary calcium score is expressed as median (interquartile range) in 18 patients. Other data are expressed as mean ± standard deviation or number (proportion, %)

Figure). We previously confirmed good interobserver agreement for SUV$_{max}$ and TBR$_{max}$ of coronary atherosclerotic lesions, and for M-TBR$_{max}$.[9,10]

Relationships Between AVC ^{18}F-NaF Uptake and Parameters of AVC and Coronary Atherosclerosis

There was no correlation between A-TBR$_{max}$ and peak aortic valve velocity on Doppler echocardiography (*r* = 0.075, *P* = 0.72). However, A-TBR$_{max}$ had a positive correlation with the AVC score (*r* = 0.54, *P* = 0.0049), density (*r* = 0.54, *P* = 0.0052), and volume (*r* = 0.52, *P* = 0.0081) (Figure 1). There was no significant difference in A-TBR$_{max}$ between patients with a history of myocardial infarction or unstable angina and those without such history (1.60 ± 0.19 vs 1.48 ± 0.17, respectively; *P* = 0.078). A-TBR$_{max}$ was similar in patients with versus without obstructive coronary stenosis (1.53 ± 0.20 vs 1.50 ± 0.17, respectively; *P* = 0.71). Patients with at least one high-risk plaque showed significantly higher A-TBR$_{max}$ than those without high-risk plaque (1.60 ± 0.18 vs 1.42 ± 0.13, respectively; *P* = 0.012) (Figure 2), whereas there were no differences in AVC parameters on CT between the two groups (AVC score: 115 [8-201] vs 74 [13-141], respectively, *P* = 0.53; AVC density: 334 Hounsfield units [181-450 Hounsfield units] vs 312 Hounsfield units [222-462 Hounsfield units], respectively, *P* = 0.98; AVC volume: 43 mm^3 [15-85 mm^3] vs 28 mm^3 [8-56 mm^3], respectively, *P* = 0.31). On multivariate analysis adjusted for age, sex, coronary risk factors, statin use, and obstructive coronary stenosis, the AVC score (β = 0.57, *P* = 0.016) and presence of high-risk plaque (β = 0.56, *P* = 0.029) were significantly correlated with increased A-TBR$_{max}$ (Table 2). Additionally, A-TBR$_{max}$ showed a positive correlation with M-TBR$_{max}$ (*r* = 0.55, *P* = 0.0043) (Figure 3).

Figure 4 shows a representative case of AVC with higher ^{18}F-NaF uptake and high-risk plaque.

Significance of ^{18}F-NaF Uptake for AVC Progression

Among the 25 patients, 11 underwent follow-up CT scan to evaluate the progression of AVC. The interval between the first and second CT scans was 35 ± 9 months. The changes in the AVC score, density, and volume were 50 (10-73), 56 Hounsfield units (17-120 Hounsfield units), and 8 mm^3 (5-18 mm^3), respectively. No significant relationship was found between A-TBR$_{max}$ and the change in AVC density (*r* = 0.35, *P* = 0.29) or volume (*r* = 0.33, *P* = 0.32). However, A-TBR$_{max}$ had a strong positive correlation with the
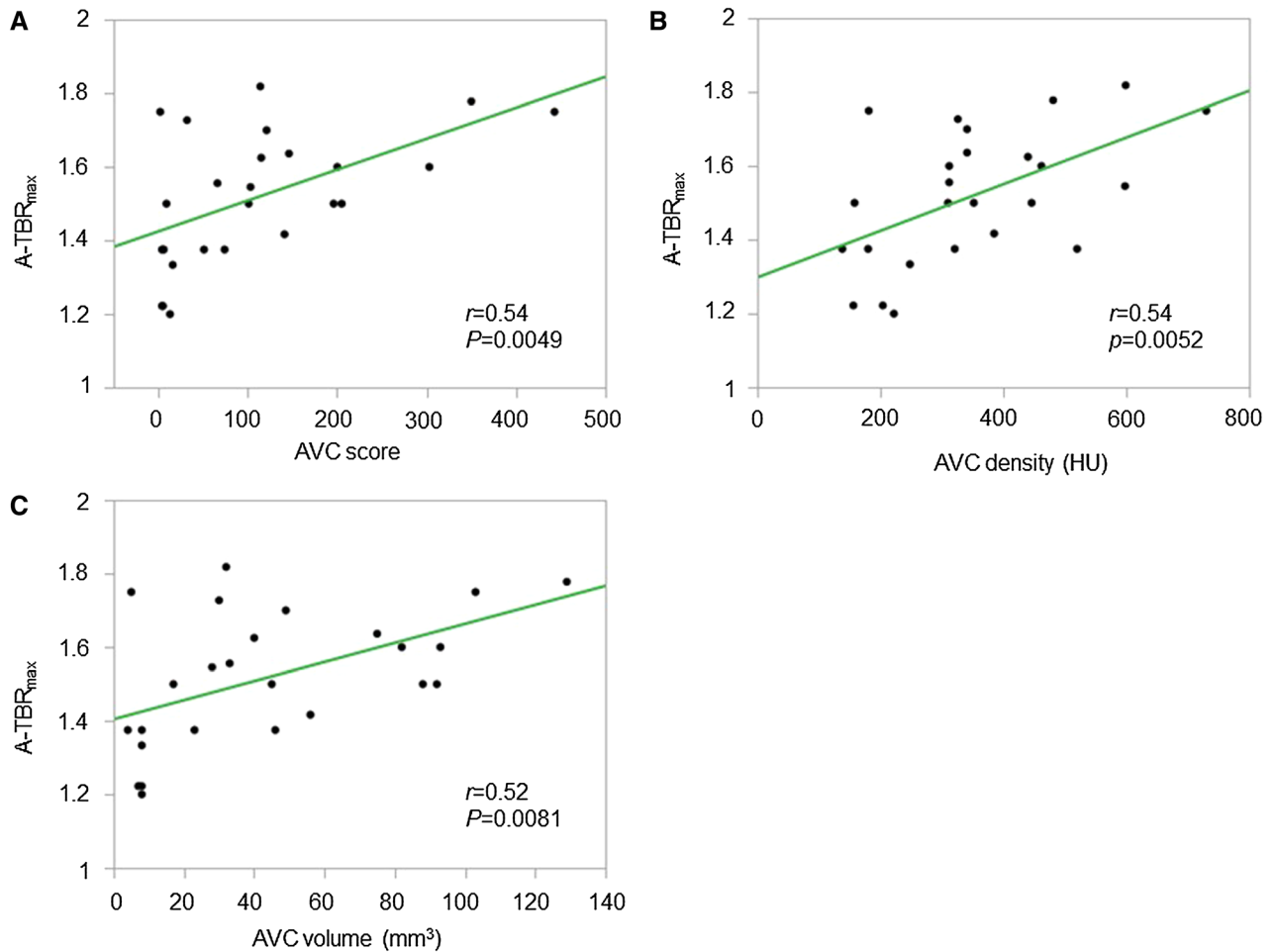
Figure 1. Relationships between ^{18}F-NaF uptake in AVC (A-TBR$_{max}$) and parameters on CT. **A-C** A-TBR$_{max}$ correlates positively with comprehensive score, density, and volume of AVC.
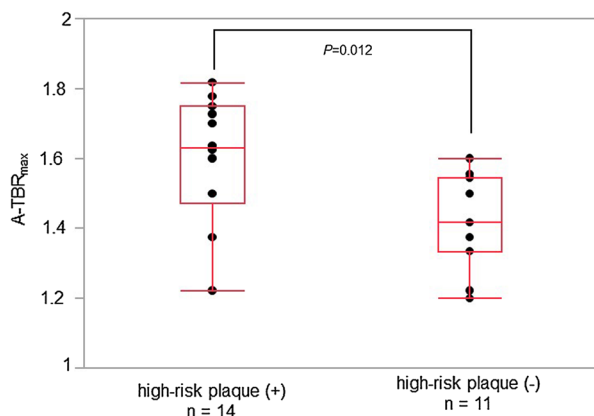

Figure 2. Comparison of ^{18}F-NaF uptake in AVC (A-TBR$_{max}$) between patients with versus without high-risk plaque on CCTA. Patients with high-risk plaque had higher A-TBR$_{max}$.

change in AVC score ($r = 0.74$, $P = 0.0091$) (Figure 5). The interval between the first and second CT scans did not correlate with the change in AVC score ($r = -0.12$, $P = 0.73$). The baseline AVC score had a moderate correlation with the change in AVC score ($r = 0.62$, $P = 0.041$).

Figure 6 shows representative cases of different levels of A-TBR$_{max}$ and AVC progression.

DISCUSSION

We investigated clinical implications of ^{18}F-NaF uptake in AVC in relation to AVC parameters (assessed with CT) and coronary atherosclerosis parameters (assessed with CT and ^{18}F-NaF PET) in patients with subclinical AVC. Additionally, we investigated the predictive value of ^{18}F-NaF uptake in AVC. We found the following: (1) ^{18}F-NaF uptake in AVC positively

Table 2. Linear regression analysis of clinical characteristics and cardiac CT findings related to ^{18}F-NaF uptake in AVC

| Variable	Univariate regression analysis		Multivariate regression analysis	
	β	P value	β	P value
Age	− 0.02	0.935		
Male sex	0.05	0.795		
Hypertension	0.17	0.410		
Dyslipidemia	− 0.03	0.883		
Diabetes mellitus	− 0.15	0.463		
Current smoking	0.22	0.301		
Statin use	− 0.04	0.843		
Obstructive coronary stenosis	0.08	0.712		
AVC score	0.54	0.005	0.57	0.016
Presence of high-risk plaque	0.49	0.012	0.56	0.029

AVC, aortic valve calcification
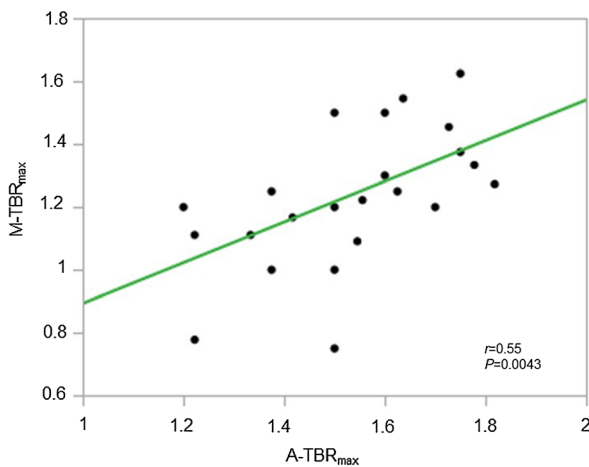
Figure 3. Correlation between ^{18}F-NaF uptake in AVC and in coronary plaque. The ^{18}F-NaF uptake in AVC (A-TBR$_{max}$) positively correlated with maximum ^{18}F-NaF uptake in coronary plaque per patient (M-TBR$_{max}$).

correlated with the calcium extent in AVC assessed with CT. (2) Increased ^{18}F-NaF uptake in AVC was related to the presence of high-risk coronary plaques on CT. (3) There was a close correlation between ^{18}F-NaF uptake in AVC and that in coronary atherosclerosis. (4) In the follow-up cohort, higher ^{18}F-NaF uptake correlated with progression of AVC. Our results indicate relationships between AVC metabolic activity and not only its calcium extent but also characteristics of coronary atherosclerosis. Greater ^{18}F-NaF uptake appears to

predict AVC progression. ^{18}F-NaF PET, as a new molecular imaging approach, may provide new information regarding biological conditions and future progression of subclinical AVC.

Many processes that drive skeletal bone formation are reported to mediate and accelerate AVC.[15-17] ^{18}F-NaF exchanges with hydroxyl groups on hydroxyapatite crystals, which are key components of both bone and tissue calcification. Thus, measurement of ^{18}F-NaF uptake allows detection of areas of developing calcification within the aortic valve. A previous study enrolling various populations with aortic sclerosis (peak aortic valve velocity < 2.0 m/s) and mild, moderate, or severe AS demonstrated that ^{18}F-NaF uptake in the aortic valve positively correlated with aortic valve calcium score on CT.[4] Our study targeted patients with AVC that did not reach clinical AS. We found positive correlations between ^{18}F-NaF uptake in AVC and calcium parameters of AVC on CT, including the comprehensive score, volume, and density. Our results indicate that ^{18}F-NaF uptake in AVC reflects details of the calcification cascade in the early stage of AVC.

The pathophysiology of AS and that of atherosclerosis are reported to share similarities.[18-20] Both conditions are initiated by endothelial damage that triggers lipid deposition and an intense inflammatory response. New AVC reportedly occurs in patients with high LDL-cholesterol and progressive atherosclerosis.[21] Our results support the theory that coronary plaques with a high lipid component and advanced positive remodeling on CT are associated with metabolically active AVC at the subclinical stage. Dweck et al. reported that ^{18}F-NaF activity in AVC was related to that in coronary
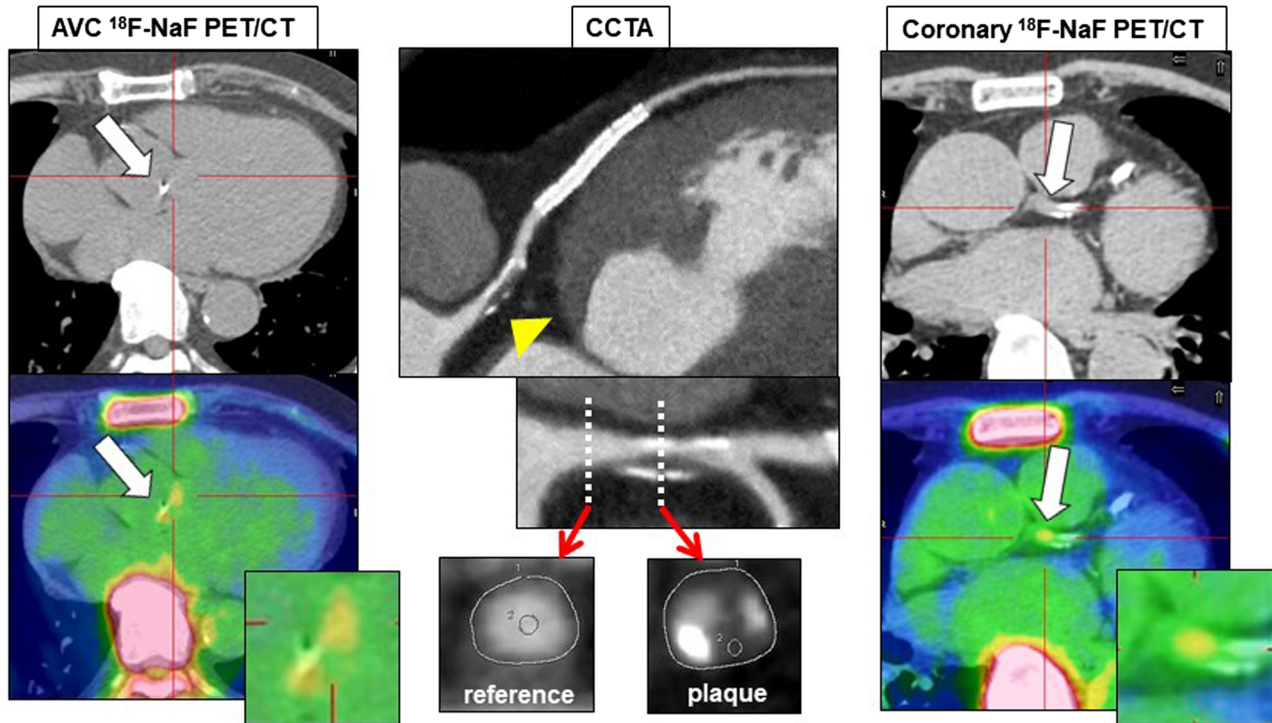
Figure 4. A representative case of enhanced ^{18}F-NaF uptake in AVC (A-TBR$_{max}$) and high-risk plaque on CCTA. The fused PET/CT image shows higher A-TBR$_{max}$ (= 1.6) (AVC ^{18}F-NaF PET/CT, arrows). The CCTA image shows high-risk plaque (minimum CT density = 22 Hounsfield units, Remodeling Index = 1.22) in the proximal portion of the left anterior descending artery (CCTA, arrowhead). Additionally, the fused PET/CT image shows enhanced ^{18}F-NaF uptake corresponding to the high-risk plaque (TBR$_{max}$ = 1.5) (coronary ^{18}F-NaF PET/CT, arrows).
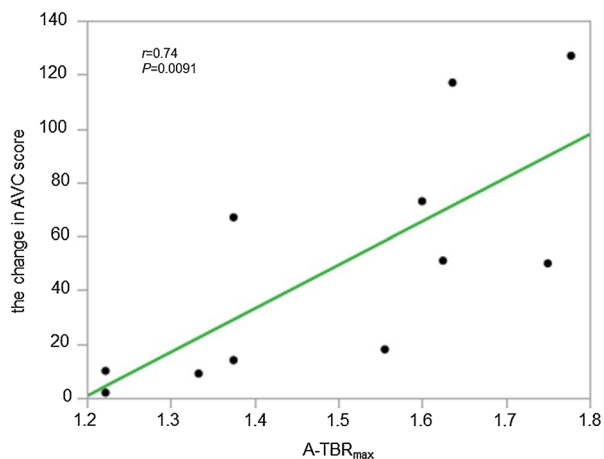

Figure 5. Correlation between ^{18}F-NaF uptake in AVC (A-TBR$_{max}$) and increase in AVC score. There was a positive correlation between these parameters.

arteries (r^2 = 0.174, P < 0.001) in various populations with aortic sclerosis and mild, moderate, or severe AS; however, the correlation was weak.[22] Despite the smaller cohort in the present study, we found a good

correlation between ^{18}F-NaF activity in AVC and patient-based maximum ^{18}F-NaF activity in coronary atherosclerosis. Our findings suggest that calcification activity of subclinical AVC and that of coronary atherosclerosis are related. We recently reported that higher ^{18}F-NaF uptake in coronary atherosclerosis had a predictive value for 2-year coronary events.[10] Simultaneous molecular assessment of AVC and coronary atherosclerosis using ^{18}F-NaF PET may be useful for comprehensive risk stratification of cardiovascular disease and may contribute to prompt therapeutic intervention in patients at high risk of cardiovascular disease.

^{18}F-NaF PET may provide a new method of predicting changes in AVC. A study of patients with AS demonstrated that valvular ^{18}F-NaF uptake correlated with histological markers of active calcification and was a good predictor of subsequent progression in aortic valve CT calcium scores at 1 year.[8] Another study demonstrated a strong correlation between baseline valvular ^{18}F-NaF uptake and the subsequent rate of progression in aortic valve calcium score.[23] Similarly, we found that baseline ^{18}F-NaF uptake in subclinical
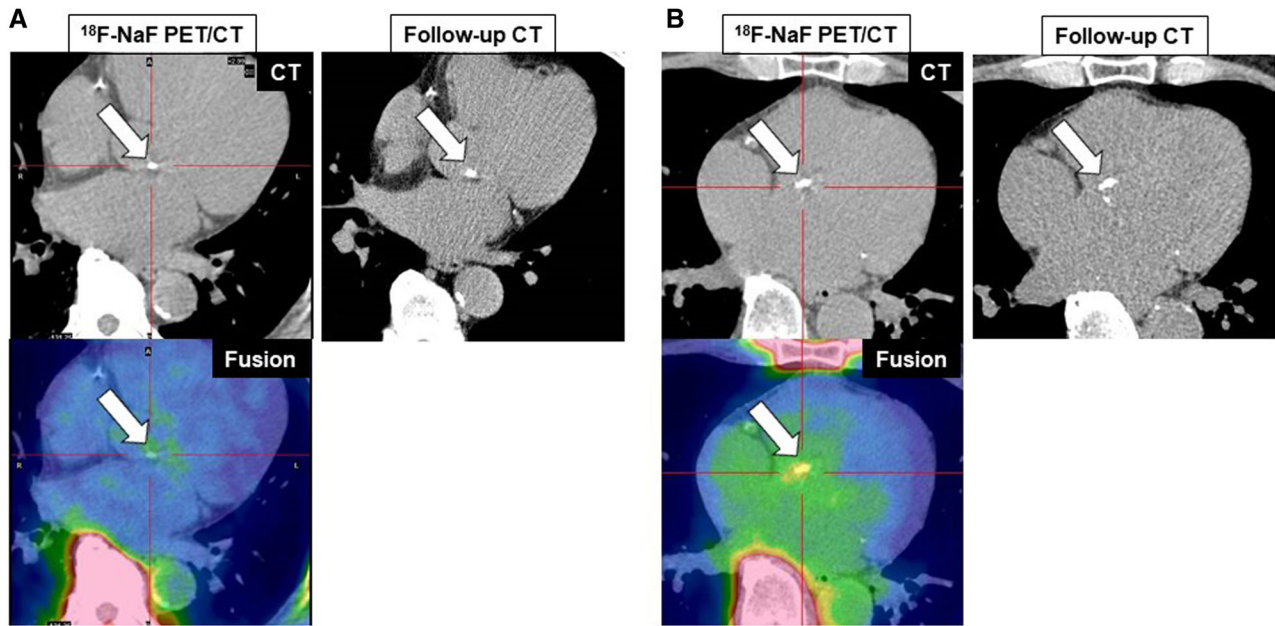
Figure 6. Representative cases showing different levels of ^{18}F-NaF uptake in AVC (A-TBR$_{max}$) and increase in AVC score. The A-TBR$_{max}$ and increase in AVC score in case A were 1.37 and 67 (51 → 118), respectively; those in case B were 1.78 and 127 (350 → 477), respectively. The interval between first and second CT scans was 35 months in both cases.

AVC had a positive correlation with the future progression of AVC. Our findings suggest that this imaging modality may allow earlier risk stratification and therapeutic intervention in patients with asymptomatic AVC. In this study, we need to take into consideration the fact that there is a wide range of intervals between the first and second CT scans. However, this factor did not correlate with the change in AVC score. Because of our small cohort, we were unable to show the incremental value of ^{18}F-NaF uptake to the baseline AVC score on CT. The relationship between the follow-up interval and change in AVC score, and the incremental value of ^{18}F-NaF uptake warrant future investigation in a larger prospective cohort.

Our study has some limitations. First, the sample size was small and we found low post hoc study powers for our nonsignificant results (e.g., differences in A-TBR$_{max}$ between patients with versus without a history of myocardial infarction or unstable angina). A larger cohort study is required to confirm the findings of this study. Second, the utility of ^{18}F-NaF uptake in aortic valves is of interest in the earlier phase before AVC is visible on CT, because ^{18}F-NaF PET provides relevant information about the state of calcified plaque before structural calcification is detectable with standard CT techniques.[24] We were not able to evaluate this aspect in this study. Additionally, we could not assess whether ^{18}F-NaF uptake in subclinical AVC predicts subsequent

changes in aortic valve function based on echocardiography and new occurrence of clinical AS from the current data. Third, there were technical limitations. The protocol for merging PET data with prior CT data and the lower resolution of PET/CT images may have caused us to miss significant signals of ^{18}F-NaF uptake in AVC and coronary arteries. A recent study demonstrated that coronary CT/PET protocol with prior CT followed by PET allowed for reliable and reproducible quantification of ^{18}F-NaF coronary uptake.[25] ^{18}F-NaF uptake can occur both at AVC sites detected on CT and remote sites from them, and the whole valve approach may be useful for avoiding missed ^{18}F-NaF activity of AVC.[26] In addition, the use of motion correction techniques could further enhance the reproducibility of image analysis,[27] and mean tissue-to-background ratio as a measure of ^{18}F-NaF uptake is potentially less prone to partial volume effect.[28] These techniques may improve clinical utility of ^{18}F-NaF PET/CT in valvular heart diseases and coronary artery diseases. Finally, we did not perform pathological assessment of AVC and coronary artery with ^{18}F-NaF uptake. Although our data suggest that calcification activity in subclinical AVC is related to characteristics of coronary atherosclerosis, this does not mean that the pathogenesis of the two conditions is similar. Indeed, several studies regarding lipid-lowering therapies, which are effective for stabilizing coronary plaque, failed to halt the progression of calcific

AS and achieve any benefit in the outcome in patients with AS.[29,30] An experimental study has reported a positive effect of statin therapy for preventing AVC progression at an early stage,[31] but we need to further examine the similarities and differences in biological mechanisms between AVC and coronary atherosclerosis.

NEW KNOWLEDGE GAINED

We have demonstrated that ^{18}F-NaF uptake in subclinical AVC is related to AVC calcium extent and high-risk coronary plaque assessed on CT and to ^{18}F-NaF uptake in coronary plaque. Higher ^{18}F-NaF uptake correlated with future progression of subclinical AVC. Our findings suggest that ^{18}F-NaF PET may provide new information regarding molecular conditions and future progression of subclinical AVC.

CONCLUSION

We demonstrate relationships between calcification activity in subclinical AVC and characteristics of coronary atherosclerosis based on ^{18}F-NaF PET and CT data. Also, our data suggest that ^{18}F-NaF uptake predicts AVC progression. ^{18}F-NaF PET may offer a new imaging option to assess molecular conditions and future progression of AVC at the subclinical stage. This study highlights the importance of further investigation in a larger cohort to determine the utility of ^{18}F-NaF PET in the management of subclinical AVC.

Acknowledgements

Disclosure

The authors declared they do not have anything to disclose regarding conflict of interest with respect to this manuscript.

References

1. Rosenhek R, Binder T, Porenta G, Lang I, Christ G, Schemper M, et al. Predictors of outcome in severe, asymptomatic aortic stenosis. N Eng J Med 2000;343:611-7.
2. Hop H, de Boer SA, Reijrink M, Kamphuisen PW, de Borst MH, Pol RA, et al. 18F-sodium fluoride positron emission tomography assessed microcalcifications in culprit and non-culprit human carotid plaques. J Nucl Cardiol 2018;26:1064-75.
3. Dweck MR, Chow MW, Joshi NV, Williams MC, Jones C, Fletcher AM, et al. Coronary arterial 18F-sodium fluoride uptake: A novel marker of plaque biology. J Am Coll Cardiol 2012;59:1539-48.
4. Dweck MR, Jones C, Joshi NV, Fletcher AM, Richardson H, White A, et al. Assessment of valvular calcification and inflammation by positron emission tomography in patients with aortic stenosis. Circulation 2012;125:76-86.
5. Aikawa E, Nahrendorf M, Figueiredo JL, Swirski FK, Shtatland T, Kohler RH, et al. Osteogenesis associates with inflammation in early-stage atherosclerosis evaluated by molecular imaging in vivo. Circulation 2007;116:2841-50.
6. New SE, Goettsch C, Aikawa M, Marchini JF, Shibasaki M, Yabusaki K, et al. Macrophage-derived matrix vesicles: An alternative novel mechanism for microcalcification in atherosclerotic plaques. Circ Res 2013;113:72-7.
7. Dweck MR, Boon NA, Newby DE. Calcific aortic stenosis: A disease of the valve and the myocardium. J Am Coll Cardiol 2012;60:1854-63.
8. Dweck MR, Jenkins WS, Vesey AT, Pringle MA, Chin CW, Malley TS, et al. 18F-sodium fluoride uptake is a marker of active calcification and disease progression in patients with aortic stenosis. Circ Cardiovasc Imaging 2014;7:371-8.
9. Kitagawa T, Yamamoto H, Toshimitsu S, Sasaki K, Senoo A, Kubo Y, et al. 18F-sodium fluoride positron emission tomography for molecular imaging of coronary atherosclerosis based on computed tomography analysis. Atherosclerosis 2017;263:385-92.
10. Kitagawa T, Yamamoto H, Nakamoto Y, Sasaki K, Toshimitsu S, Tatsugami F, et al. Predictive value of 18F-sodium fluoride positron emission tomography in detecting high-risk coronary artery disease in combination with computed tomography. J Am Heart Assoc 2018;7:e010224.
11. Raff GL, Abidov A, Achenbach S, Berman DS, Boxt LM, Budoff MJ, et al. SCCT guidelines for the interpretation and reporting of coronary computed tomographic angiography. J Cardiovasc Comput Tomogr 2009;3:122-36.
12. Allison MA, Cheung P, Criqui MH, Langer RD, Wright CM. Mitral and aortic annular calcification are highly associated with systemic calcified atherosclerosis. Circulation 2006;113:861-6.
13. Motoyama S, Kondo T, Sarai M, Sugiura A, Harigaya H, Sato T, et al. Multislice computed tomographic characteristics of coronary lesions in acute coronary syndromes. J Am Coll Cardiol 2007;50:319-26.
14. Motoyama S, Sarai M, Harigaya H, Anno H, Inoue K, Hara T, et al. Computed tomographic angiography characteristics of atherosclerotic plaques subsequently resulting in acute coronary syndrome. J Am Coll Cardiol 2009;54:49-57.
15. Mohler ER 3rd, Gannon F, Reynolds C, Zimmerman R, Keane MG, Kaplan FS. Bone formation and inflammation in cardiac valves. Circulation 2001;103:1522-8.
16. Rajamannan NM, Subramaniam M, Rickard D, Stock SR, Donovan J, Springett M, et al. Human aortic valve calcification is associated with an osteoblast phenotype. Circulation 2003;107:2181-4.
17. Aksoy Y, Yagmur C, Tekin GO, Yagmur J, Topal E, Kekilli E, et al. Aortic valve calcification: Association with bone mineral density and cardiovascular risk factors. Coron Artery Dis 2005;16:379-83.
18. O'Brien KD, Reichenbach DD, Marcovina SM, Kuusisto J, Alpers CE, Otto CM. Apolipoproteins B, (a), and E accumulate in the morphologically early lesion of 'degenerative' valvular aortic stenosis. Arterioscler Thromb Vasc Biol 1996;16:523-32.
19. Olsson M, Thyberg J, Nilsson J. Presence of oxidized low density lipoprotein in nonrheumatic stenotic aortic valves. Arterioscler Thromb Vasc Biol 1999;19:1218-22.

20. Otto CM, Kuusisto J, Reichenbach DD, Gown AM, O'Brien KD. Characterization of the early lesion of 'degenerative' valvular aortic stenosis. Histological and immunohistochemical studies. Circulation 1994;90:844-53.

21. Messika-Zeitoun D, Bielak LF, Peyser PA, Sheedy PF, Turner ST, Enriquez-Sarano M, et al. Aortic valve calcification: Determinants and progression in the population. Arterioscler Thromb Vasc Biol 2007;27(3):642-8.

22. Dweck MR, Khaw HJ, Sng GK, Luo EL, Baird A, Williams MC, et al. Aortic stenosis, atherosclerosis, and skeletal bone: Is there a common link with calcification and inflammation? Eur Heart J 2013;34:1567-74.

23. Jenkins WS, Vesey AT, Shah AS, Pawade TA, Chin CW, White AC, et al. Valvular (18)F-fluoride and (18)F-fluorodeoxyglucose uptake predict disease progression and clinical outcome in patients with aortic stenosis. J Am Coll Cardiol 2015;66:1200-1.

24. Beheshti M, Saboury B, Mehta NN, Torigian DA, Werner T, Mohler E, et al. Detection and global quantification of cardio-vascular molecular calcification by fluoro18-fluoride positron emission tomography/computed tomography—A novel concept. Hell J Nucl Med 2011;14:114-20.

25. Kwiecinski J, Adamson PD, Lassen ML, Doris MK, Moss AJ, Cadet S, et al. Feasibility of coronary 18F-sodium fluoride posi-tron-emission tomography assessment with the utilization of previously acquired computed tomography angiography. Circ Cardiovasc Imaging 2018;11:e008325.

26. Pawade TA, Cartlidge TR, Jenkins WS, Adamson PD, Robson P, Lucatelli C, et al. Optimization and reproducibility of aortic valve 18F-fluoride positron emission tomography in patients with aortic stenosis. Circ Cardiovasc Imaging 2016;9:e005131.

27. Massera D, Doris MK, Cadet S, Kwiecinski J, Pawade TA, Peeters FECM, et al. Analytical quantification of aortic valve 18F-sodium fluoride PET uptake. J Nucl Cardiol 2019. https://doi.org/10.1007/s12350-018-01542-6.

28. Cal-Gonzalez J, Li X, Heber D, Rausch I, Moore SC, Schäfers K, et al. Partial volume correction for improved PET quantification in 18F-NaF imaging of atherosclerotic plaques. J Nucl Cardiol 2018;25:1742-56.

29. Cowell SJ, Newby DE, Prescott RJ, Bloomfield P, Reid J, Northridge DB, et al. A randomized trial of intensive lipid-low-ering therapy in calcific aortic stenosis. N Eng J Med 2005;352:2389-97.

30. Rossebø AB, Pedersen TR, Boman K, Brudi P, Chambers JB, Egstrup K, et al. Intensive lipid lowering with simvastatin and ezetimibe in aortic stenosis. N Eng J Med 2008;359:1343-56.

31. Rajamannan NM, Subramaniam M, Stock SR, Stone NJ, Springett M, Ignatiev KI, et al. Atorvastatin inhibits calcification and enhances nitric oxide synthase production in the hypercholes-terolaemic aortic valve. Heart 2005;91:806-10.